



Contents lists available at ScienceDirect

International Journal of Sediment Research

journal homepage: www.elsevier.com/locate/ijsrc

Original Research

Using Cs-137 measurements and RUSLE model to explore the effect of land use changes on soil erosion and deposition rates in a mid-sized catchment in southern Italy

Paolo Porto ^{a, b, *}, Giovanni Callegari ^c, Abid Ouadja ^d, Ernesto Infusino ^e^a Department of Agraria, University Mediterranea of Reggio Calabria, 89123 Reggio Calabria, Italy^b Faculty of Geographical Sciences, Kazimierz Wielki University, 85-033 Bydgoszcz, Poland^c Consiglio Nazionale delle Ricerche (CNR) - Istituto per i Sistemi Agricoli e Forestali del Mediterraneo (ISAFOM), Italy^d Department of Agronomy, University of Mascara, BP305, 29000 Mascara, Algeria^e UNICAL - Dipartimento di Ingegneria per l'Ambiente, Territorio e Ingegneria Chimica (DIATIC), Italy

ARTICLE INFO

Article history:

Received 29 May 2023

Received in revised form

17 October 2023

Accepted 8 November 2023

Available online xxx

Keywords:

Soil loss

Sediment deposition

Revised Universal Soil Loss Equation

(RUSLE)

Cesium-137

Italy

ABSTRACT

In some areas of southern Italy, the change in land use over the last 4–5 decades has increased pressure on land and water resources and caused different forms of soil degradation. In order to mitigate the magnitude of soil erosion, different strategies that include construction of flood control structures and reforestation programs have been done in several areas. However, quantifying the effectiveness of these strategies is difficult in absence of direct measurements of soil erosion. To cover this information gap, the use of distributed numerical models coupled with measurements of the radionuclide cesium-137 (¹³⁷Cs) offers a good alternative to the classic experimental sites (plot, catchments) that, on the contrary, require long term datasets to produce reliable estimates of soil loss. In this paper, measurements of ¹³⁷Cs in a floodplain area are firstly described for a representative Calabrian catchment as an example to reconstruct the trend of soil deposition rates during the last six decades. These measurements have been integrated with estimates of soil loss obtained with the Revised Universal Soil Loss Equation (RUSLE) model for which land use maps of different periods are available. The final comparison between estimates of soil erosion provided by the RUSLE at catchment scale and sedimentation rates derived from ¹³⁷Cs measurements on depositional areas allowed interesting information on the trend of soil erosion and deposition rates in these areas to be obtained.

© 2023 International Research and Training Centre on Erosion and Sedimentation/the World Association for Sedimentation and Erosion Research. Published by Elsevier B.V. All rights reserved.

1. Introduction

Soil erosion by water is a very important threat that affects human activities and has negative implications for the world economy (Panagos et al., 2018; Pimentel et al., 1995). The main drivers of increased soil erosion are generally recognized as changes in land use (Moustakim et al., 2019; Senanayake et al., 2020; Uddin et al., 2019), consisting mainly of reduction of forested areas replaced by cultivations (Maeda et al., 2010), occurrence of urban sprawl (Hu et al., 2001; Shao et al., 2021) connected to the abandonment of marginal lands (Arnaez et al., 2011; Romero Diaz et al., 2017), and, in several cases, climate change, consisting of a general increase of rainfall intensity and frequency and of the

occurrence of heavier precipitation events (Capra et al., 2017; Li & Fang, 2016; Nearing et al., 2004). All these natural or anthropic factors generate values of soil loss of high magnitude especially in vulnerable areas. In these areas, high values of soil loss produce a large amount of sediment transported downstream through the river system that may cause negative effects which mainly include loss of soil productivity (Lal & Moldenhauer, 1987), inundation of floodplain areas (Robinson & Blackman, 1990), and reduction of water storage in reservoirs (De Vincenzo et al., 2017).

In some areas of Calabria, southern Italy, soil erosion by water is particularly severe. Porto et al. (2018), for example, based on direct observations over small uncultivated catchments, documented very high rates of sediment yield (around 100–150 t/(ha·y)) during the last few decades. These rates are not uncommon even in cultivated sites of the region where traditional cropping systems revealed the fragility of the upland areas (see Porto et al., 2022).

* Corresponding author.

E-mail address: paolo.porto@unirc.it (P. Porto).

In order to reduce the amount of soil loss and to prevent phenomena of sedimentation downstream, land use changes consisting of long-term programs of reforestation have been applied as the most appropriate means of mitigating erosion risk in Calabria (Altieri et al., 2018; Khodadadi et al., 2020; Porto et al., 2009). Important examples in this direction were the activities done after big floods occurred in Calabria in 1951 and 1953. Calculations, made after those floods, documented economic losses of around 15.5 million Euros for Calabria, Sardinia, and Sicily (Lastoria et al., 2006) and gave important input to revise the national and local legislation in the field of torrential flood control. In those cases, the “Special Law” 1177/55 of November 26, 1955, the public work projects in the 1950s provided by the “Cassa per il Mezzogiorno” (established by the national government in 1950 to encourage the development of public works and infrastructure of southern Italy), and the “Soil Conservation Project” proposed by the National Research Council of Italy (CNR) are important programs that concurred to promote a massive activity of reforestation within the region. Following these programs, more than 160,000 ha of the whole region were stabilized by reforestation and landslide protection from the early '50s to the late '70s (D'Ippolito et al., 2013; Scarciglia et al., 2020).

However, despite the intense soil conservation activities applied in that period, the absence of direct measurements of soil erosion during the last 4–5 decades makes it difficult to establish the effects of the control strategies in these areas. The need to assess soil erosion risk and to establish the effectiveness of these strategies for controlling land degradation has directed attention to the use of distributed numerical models, coupled with geographical information systems (GIS), to provide predictions of soil erosion in large areas. In this context, the use of Revised Universal Soil Loss Equation (RUSLE) model (Renard et al., 1994) to predict long-term estimates of soil loss proved to be very effective in many countries throughout the world including Italy (Di Stefano et al., 2000; Porto et al., 2022; Terranova et al., 2009). However, the limitations of the RUSLE model to provide information on deposition rates requires a complementary technique able to account for soil accumulation in the sedimentation areas (Di Stefano et al., 2005; Porto & Walling, 2015).

During the last decades, measurements of cesium-137 (^{137}Cs) in reservoirs and in floodplain areas have proven to be very effective to obtain reliable estimates of soil deposition rates at long-term temporal scales (Froehlich & Walling, 2007; Golosov et al., 2013; He & Walling, 1996; Ritchie et al., 1975). The ^{137}Cs (half-life of around 30 years) is a manmade radiotracer that was produced mainly by the nuclear tests established from the early 1950s to the late 1970s and

that came to the ground by atmospheric deposition (fallout). Additional ^{137}Cs fallout also is detected in many countries of Europe as a result of the Chernobyl accident in 1986. In Italy, information on the mean ^{137}Cs deposition flux over the country is reported by ISIN (2021) and it is replotted in Fig. 1 (see also Porto & Callegari, 2022).

The yearly record in Fig. 1 shows, for the period covered by the nuclear tests, a maximum fallout in 1963 with another distinctive peak in 1959. The 1963 peak is followed by a slow, progressive decrease until 1985. In 1986, another distinctive peak, with a value of around 6,000 Bq/m², can be seen as Chernobyl-related ^{137}Cs fallout; after that, a rapid decline until 1994, when the radiation levels have rapidly returned to normal, can be observed.

According to Ritchie et al. (1973), the ^{137}Cs deposited in a sediment profile is closely related to the fallout rate at a given location, because most ^{137}Cs accumulated on the sedimentation area is transported by the suspended material through the fluvial system and, as such, it reflects the historical flood record of the catchment. Based on the foregoing assumption, the ^{137}Cs peak in a sediment profile should be associated with the peak rate of the ^{137}Cs atmospheric fallout and it can be used as a “marker horizon” for that profile. Using this strategy, a temporal sediment deposition pattern can be derived for different time windows that extend from the beginning of fallout (1954) to the years (1959, 1963, 1986) marked by the peak rates of ^{137}Cs atmospheric fallout. The date of sampling will finally mark the total deposition depth from the last marker horizon (1986) to the collection time.

The purpose of the current study is to make use of the ^{137}Cs technique to document the sediment deposition patterns in the floodplain area adjacent to a representative Calabrian catchment (Italy), for which detailed information on land use change, soil, topography, and climate also is available. As a first step, measurements of ^{137}Cs obtained from three sampling points located on a floodplain area were used to provide information on sedimentation rates in this area. Then, a distributed approach able to provide soil loss estimates for different periods has been applied using the RUSLE model. The temporal trends of the resulting estimates of both sediment deposition and soil loss are then compared.

2. Material and methods

2.1. Study area

The study area is located in Calabria, southern Italy, and it is represented by the Crati catchment, closed at Tarsia Dam (1,332 km²)

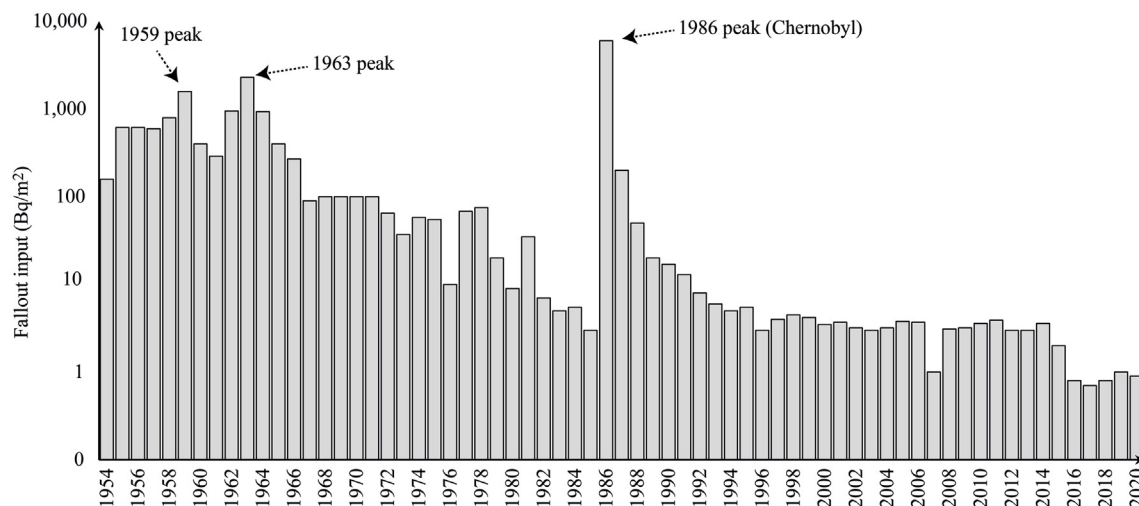


Fig. 1. ^{137}Cs deposition flux in Italy (mean values for the country) from 1954 to 2020 (from ISIN, 2021; replotted).

(Fig. 2). The Crati catchment, with a boundary length of 257 km and the length of the main river channel of ca. 71.4 km, is the largest catchment in Calabria. From a morphological point of view, two main reliefs can be distinguished in the catchment: the first one, the Sila Plateau, is orientated to the West, and the second one, the Coastal Chain, faces the East (see the digital elevation model in Fig. 2).

The mean elevation is around 672 m a.s.l., with the maximum located at the Sila Plateau (1,856 m a.s.l.), and the minimum at the Tarsia Dam (49 m a.s.l.). Based on the long-term data provided by 14 temperature and 21 precipitation recording stations, the climate of the area can be classified as sub-humid (Thornthwaite, 1948). The mean annual rainfall accounts for around 1,200 mm, mainly occurring during the period extending from October to March, and the mean annual temperature is around 11.9 °C (ranging from a minimum of 4.1 °C in January to a maximum of 20.7 °C in July and August).

Geologically, the catchment is a Pleistocene-Holocene extensional basin filled by clastic marine and fluvial deposits (Formetta et al., 2014). It is characterized by the presence of areas underlain by several contrasting rock types that range from plutonic and metamorphic crystalline rocks in the Sila Massif, to sedimentary and crystalline rocks in the Coastal Chain and to carbonate and siliciclastic sedimentary rocks in the Pollino group (Amodio Morelli et al., 1976; Cello et al., 1981; Vespasiano et al., 2014). The main soil types also are contrasting and range from poorly to moderately differentiated soils, such as Cambisols and Leptosols, to more developed Vertisols and Luvisols (Soil Survey Staff, 2014). These are characterized by a large range of textures, although sandy and silt-sandy soils are dominant (ARSSA, 2003).

Large areas of the catchment (~36%) are cultivated but the dominant part (~56%) is covered by trees, which include primarily pines (*Pinus laricio*), the peculiar feature of the forested landscape in the Sila Massif, but also some other conifers like Douglas-fir (*Pseudotsuga menziesii* Mirb) and Monterey pine (*Pinus radiata* D. Don), some broadleaves species like Turkey oak (*Quercus cerris* L.), chestnut (*Castanea sativa* Mill.), beech (*Fagus sylvatica* L.), and some stands of alder, willow, and aspen along the river corridors. The remaining portion (~8% of the catchment area) supports original rangeland with grass and scrub vegetation and urban areas. In the early 1920s, a long-term campaign of measurements able to provide information on the suspended sediment loads of the River Crati, has been undertaken. A location at the "Strette di Tarsia", along the main course of the river, was identified as the preferred site for a dam useful for the irrigation of the entire Sibari plain and the area nearby. The dam was completed in 1959 and it operates during the period from April to October following the end of the rainy season. In 1990, the Calabria Region approved the establishment of a protected area around the lake which represents to date an area of considerable naturalistic interest due to the existence of numerous ecosystems of value and for the great variety of plant and animal species.

2.2. Sediment sampling campaign for ^{137}Cs measurements

The sampling campaign was undertaken in January 2021 and aimed at documenting the ^{137}Cs depth distribution in sediment cores collected from the floodplain area, in order to provide information on the sedimentation rate of the catchment. Sampling within the area covered by the reservoir was not possible at a short distance from the dam because the area is under protection of a regional law. However, a floodplain along the river, located just outside the boundary of the protected area (Fig. 3), was identified as a deposition site representative of the entire catchment.

Sectioned cores were collected from three different locations using an 11 cm diameter steel core tube driven into the sediment to a depth of ~200 cm, by a percussion driver. Care was taken in

identifying the areas of the floodplain where sedimentation occurred during the last decades. This operation was possible thanks to the availability of aerial photos for different periods. The resulting cores were sectioned at depth increments of 2 cm, to a depth of ~100 cm and of 4 cm to a depth of ~200 cm. A total of 230 individual samples were analyzed for ^{137}Cs measurements.

2.3. Laboratory analyses

Each sample was oven dried at 105 °C for 48 h, disaggregated and dry sieved to separate the < 2 mm fraction. A representative sub-sample of this fraction was placed into a Petri dish for determination of ^{137}Cs activity by gamma spectroscopy. All the samples were measured using two Canberra p-type high-resolution low energy coaxial high purity germanium (HPGe) detectors (model GX4020) with a relative efficiency of 45%. The detectors are calibrated using the software Laboratory Sourceless Calibration Software (LABSOCS) and a multigamma source. For all the samples, a counting time ranging from about 80,000 to about 240,000 s was applied depending on the expected activity. The activity (Bq/kg) for each sample was obtained from the counts at the 662 keV peak in the measured γ -ray spectrum. The ^{137}Cs measurements have been standardized to a fixed date at the end of 2020. This choice was motivated by the need to exclude the year 2021 from the counting because the sampling campaign was made in mid-January and no significant rainfall events occurred in the area during the first two weeks of 2021.

2.4. Input parameters for applying the RUSLE model

In the absence of direct observations of soil loss, the RUSLE model was applied to the test catchment in the version proposed by Renard et al. (1994) that can be expressed by Eq. (1):

$$A = R \cdot K \cdot LS \cdot C \cdot P \quad (1)$$

where A (t/(ha·y)) is the mean value of soil loss related to the investigated period; R is the rainfall erosivity factor related to the same time window (MJ·mm/(ha·h·y)); K (t·ha·h/(ha·MJ·mm)) is the soil erodibility factor (Wischmeier et al., 1971); LS (dimensionless) is the topographic factor (McCool et al., 1987, 1989; Renard et al., 1994); C (dimensionless) is the cover and management factor related to the investigated period (Wischmeier & Smith, 1978); and P (dimensionless) is the support practice factor. Long-term measurements of the rainfall erosivity factor R were necessary to generate a map of the isoerodent values for the study area (see Porto, 2016). More specifically, 16 rainfall stations (see Table 1), for which measurements of rainfall at short time interval (30 min) were available for at least 20 years, were used to produce the isoerodent map of Fig. 4. The calculation of R for each station was made using the equations provided by Wischmeier and Smith (1978) and the spatial interpolation over the catchment area was produced by a kriging procedure.

The information necessary to produce an equivalent map of the soil erodibility factor K has been derived from a detailed soil map of Calabria that allowed the combination of soil texture, structure, permeability, and organic matter content (see ARSSA, 2003). A map of K was obtained by combining this information and it is shown in Fig. 5.

A digital elevation model (DEM) with a regular 20 m grid was used to derive the spatial distribution of both the topographic factor LS and the P -factor for the catchment area. More specifically, the DEM was preliminarily imported into the SAGA GIS (<http://www.saga-gis.org>, version: 7.5.0) and the spatial distribution of the topographic factor LS was obtained using the Moore and Burch

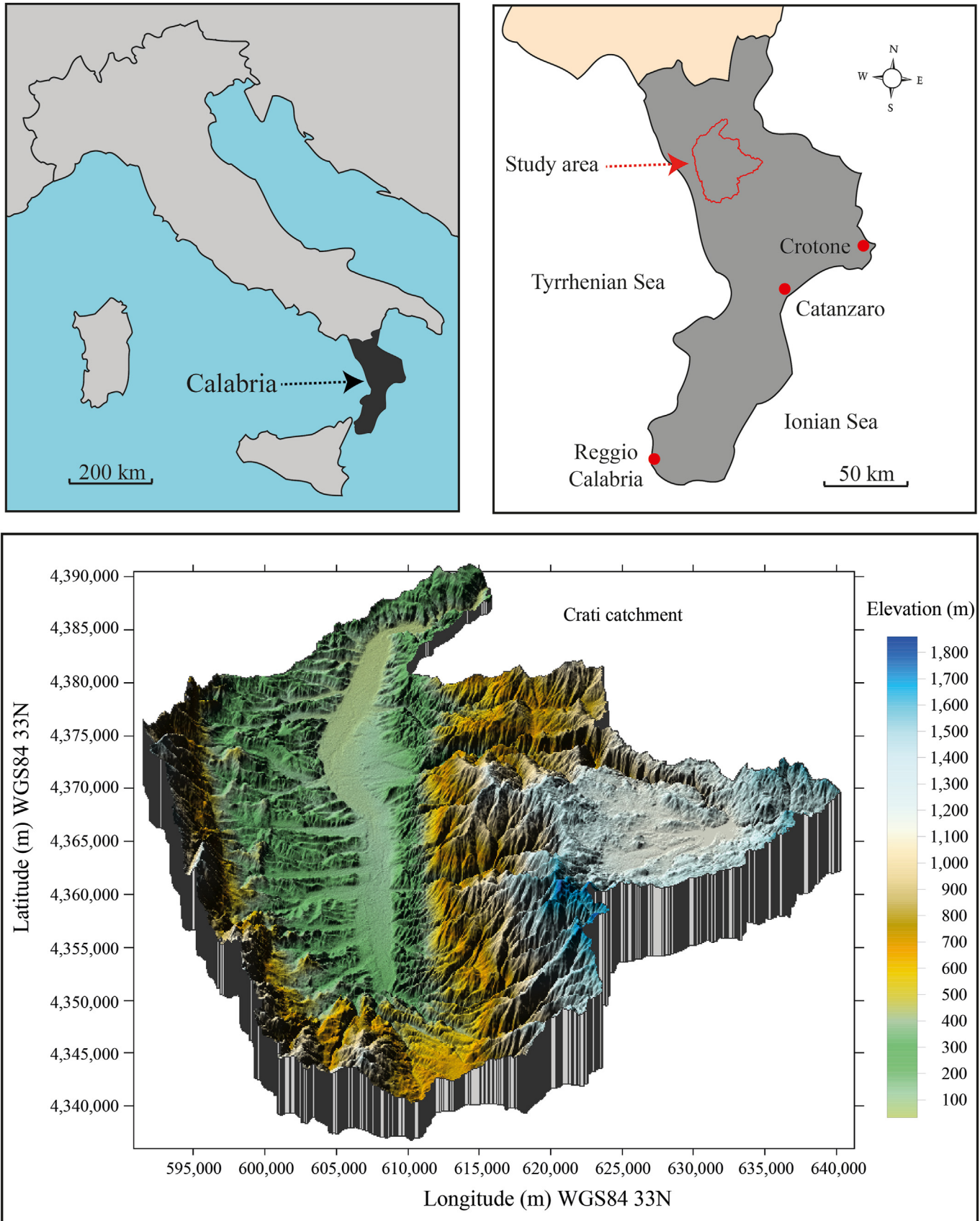


Fig. 2. Study area and representative catchment.

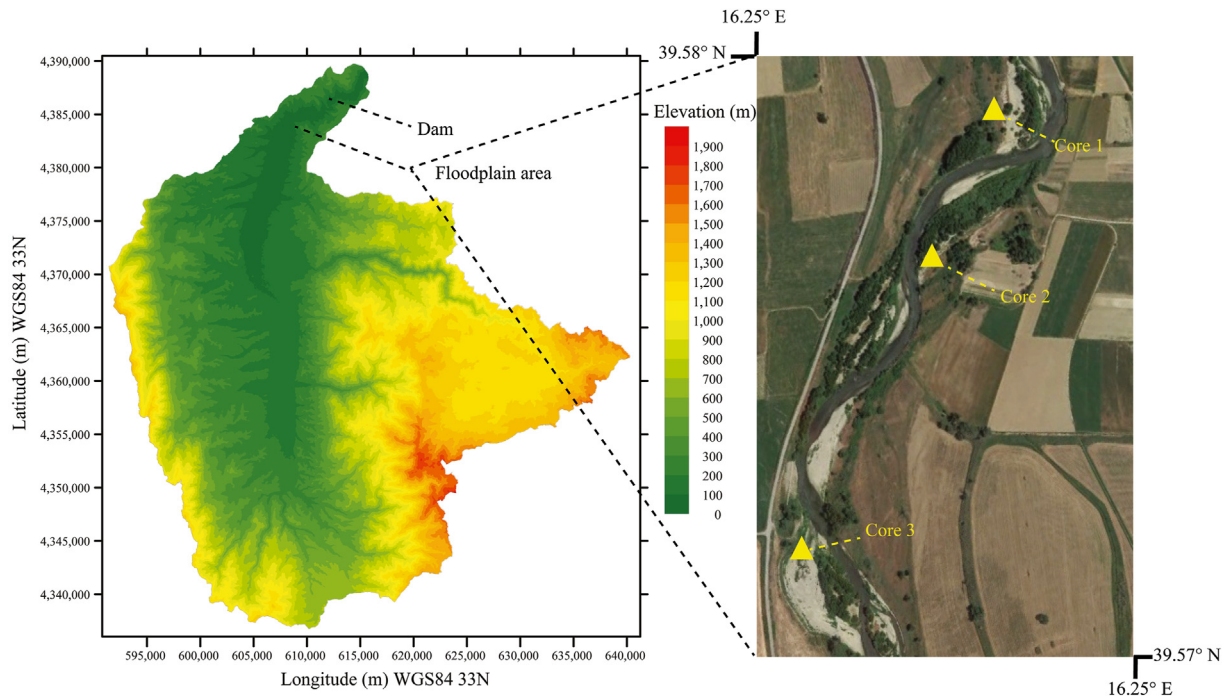


Fig. 3. Elevation map of the Crati catchment (left) and the sampling points in the floodplain area (right).

(1986) calculation routine. The spatial distribution of P was derived by combining the values of slope and the land use map. The resulting maps are shown in Figs. 6(a) and 6(b).

In order to investigate the trend of soil loss for different periods following the reforestation activities, it was necessary to provide information of changes in land use over long time windows. To this purpose, satellite images provided by Landsat 1–7 imagery from 1977 to 2010, and the land use maps derived by the Corine Land Cover 1990, 2000, and 2012 projects, were used to calculate the spatial distribution of the cover and management factor, C , for different periods. More specifically, satellite images (with a resolution of 28.5, 50, and 57 m, depending on the year) were acquired from the U.S. Geological Survey (USGS) website (<https://earthexplorer.usgs.gov/>) for the years 1977, 1999, and 2010. These years were selected as they reflect the retrospective information of

the main changes in land use that have occurred in the area from the beginning of reforestation to the age of maturity of the trees. To determine the C factor from remote sensing data, the method based on the normalized difference vegetation index (NDVI), calculated as a ratio of red (R) band and near-infrared (NIR) band values was applied, which reflects the fraction of photo-synthetically active radiation absorbed (Ouardja et al., 2021; Sahli et al., 2019). The results of this calculation are reported on the maps shown in Figs. 7(a)–7(c), that indicate the spatial distribution of the C -factor for the years 1977, 1999, and 2010.

All the foregoing maps (R , K , LS , P , and C) were imported into SURFER (<https://www.goldensoftware.com/products/surfer>, trial version: 16.5.446) to obtain three different scenarios of soil loss using Eq. (1).

Table 1

Rainfall stations used for calculation of the R -factor. Geographic location of each station is expressed in coordinates World Geodetic System 1984/UTM zone 33N. Area of use: between 12°E and 18°E, northern hemisphere between equator and 84°N, onshore and offshore.

Code	Station	COORD WGS84 33N		Elevation (m a.s.l.)
		(m)	(m)	
1	Aciri	618,872.713	4,371,766.98	674
2	Camigliatello Monte Curcio	621,931.891	4,352,947.12	1,509
3	Cecita ex Acquacalda	632,874.306	4362,095.37	1,166
4	Cosenza	609,018.132	4,349,467.85	249
5	Montalto Uffugo	599,782.170	4,362,432.41	430
6	Tarsia	609,256.054	4,386,056.35	187
7	Torano Scalo	604,034.270	4,372,277.68	99
8	Cetraro Superiore	580,758.565	4,374,605.56	64
9	Fiumefreddo Bruzio	592,040.39	4,343,467.02	195
10	Macchia Albanese	618,642.008	438,124.47	425
11	Malvito	590,394.947	4,383,777.08	423
12	Nocelle	633,697.008	4,344,808.93	1,301
13	Paola	589,759.662	4,358,053.49	142
14	Rogliano	614,001.862	4,337,157.87	630
15	San Sosti	588,171.672	4,391,009.48	419
16	Schiavonea	632,054.772	4,390,422.66	1

3. Results

3.1. ^{137}Cs depth distribution for the sectioned cores in the floodplain area and the associated sedimentation rates

The activities of ^{137}Cs along the sediment deposit associated with the three sampling points indicated in Fig. 2 are shown in Fig. 8. As indicated previously, the core samplers were inserted into the ground to a total depth of ~200 cm. It is worth noting that no ^{137}Cs activity was found below a depth of about 180 cm. This evidence was confirmed by further bulk samples collected at deeper depths (200–240 cm) from the same pits. These additional samples showed no ^{137}Cs content in deeper layers and this indicates that, in the investigated area, the total ^{137}Cs activity is included in the first 180 cm. In view of these findings, the profiles shown in Fig. 8 are expected to show all the ^{137}Cs atmospheric flux since the beginning of fallout in 1954 to the date of sampling. This suggests that, even if the construction of the reservoir dates back to 1959, its impoundment did not affect the deposition processes in the floodplain area because the sampling points are located sufficiently far upstream of the reservoir.

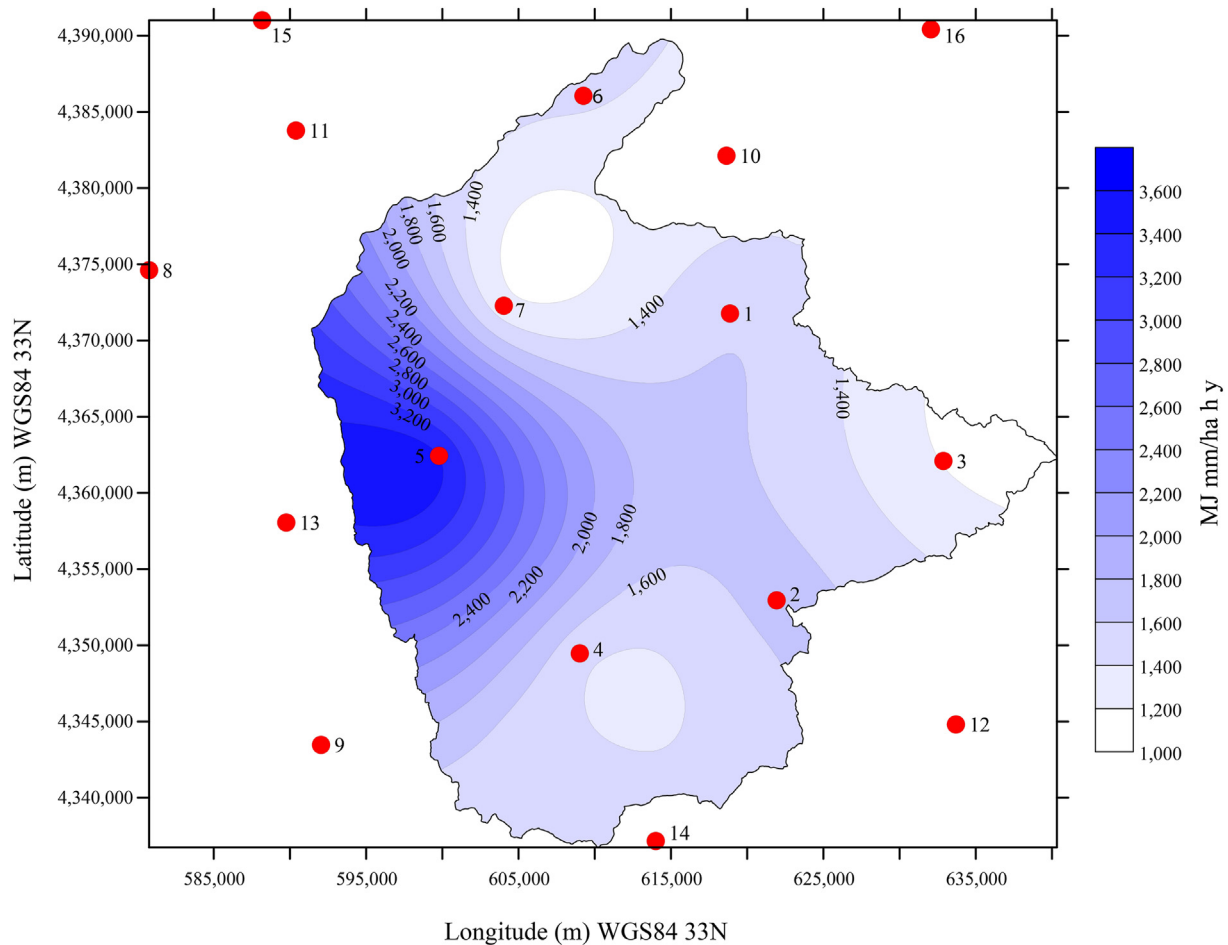


Fig. 4. Iso-erodent map for the study area and the rainfall stations used for calculations.

A first visual inspection of the profiles in Fig. 8 indicates evidence of the 1963 peak in ^{137}Cs activity at a similar mass depth (1,200–1,300 kg/m^2) and suggests to use this as a first marker horizon. In other words, the current depth of this peak allows an estimate of the sedimentation rate between 1963 and the time of sampling at the point where the core was collected (see Zapata et al., 2002). Based on the depth distribution obtained from Site 1, the peak of ^{137}Cs concentration can be identified at a mass depth of 1,259 kg/m^2 and this can be related to the 1963 peak in atmospheric fallout. Equally, from Site 2, the same peak can be associated with a mass depth of 1,241 kg/m^2 and from Site 3 at 1,258 kg/m^2 . Information on the sedimentation rate can be obtained from the depth of sediment above the ^{137}Cs peak, which denotes the reservoir surface in 1963, using Eq. (2) (Porto et al., 2016):

$$R' = \frac{M}{T} \quad (2)$$

where R' is the rate of deposition ($\text{kg}/(\text{m}^2 \cdot \text{y})$); M is the cumulative mass depth of the 1963 peak (kg/m^2); and T is the time elapsed between 1963 and the sampling campaign (y).

The three estimates of deposition rate obtained for the cores collected in the floodplain area, for the time window 1963–2020, are listed in Table 2.

The three profiles in Fig. 8 show, also, a second peak of ^{137}Cs activity in the upper ca. 20–40 cm of the cores which can be related to the Chernobyl fallout in 1986 (see Belyaev et al., 2013a; Golosov et al., 2013). It is worth noting that in two cases, for Site 2 and Site 3, the second peak shows a ^{137}Cs activity (4.2 and 5.3 Bq/kg,

respectively) lower than that documented by the 1963 peak (7.6 and 8.4 Bq/kg, respectively). On the contrary, for Site 1, the ^{137}Cs activity related to 1986 (9.8 Bq/kg) is higher than that associated to the 1963 peak (6.2 Bq/kg). Although it is difficult to provide a definitive explanation for these different values, it is important to recognize that the spatial variability of the Chernobyl flux in this catchment may have affected the sediment deposited in the floodplain area. For example, the sediment deposited at Site 1 may be generated from areas of the catchment that received a higher flux and this would explain the higher activity in the signal. A second, possible explanation, can be related to the chance that this sediment may derive from upper layers of reforested soils that were the major contributors prior to reforestation and that are now richer in ^{137}Cs activity in the upper horizons.

Nevertheless, the presence of the Chernobyl signal in the three cores suggests to use this peak as a second marker horizon which denotes the floodplain surface in 1986. Eq. (2) was applied, again, to obtain the rates of sedimentation for the three sampling points for the time window 1986–2020, which is listed in Table 2 as well.

3.2. Estimates of soil loss provided by the RUSLE model for three different scenarios of land use

The application of the RUSLE model as per Eq. (1) was done using SURFER. This software required the use of the maps previously described at the same mesh size. Because the resolution of the original maps was different, it was necessary to rescale them to

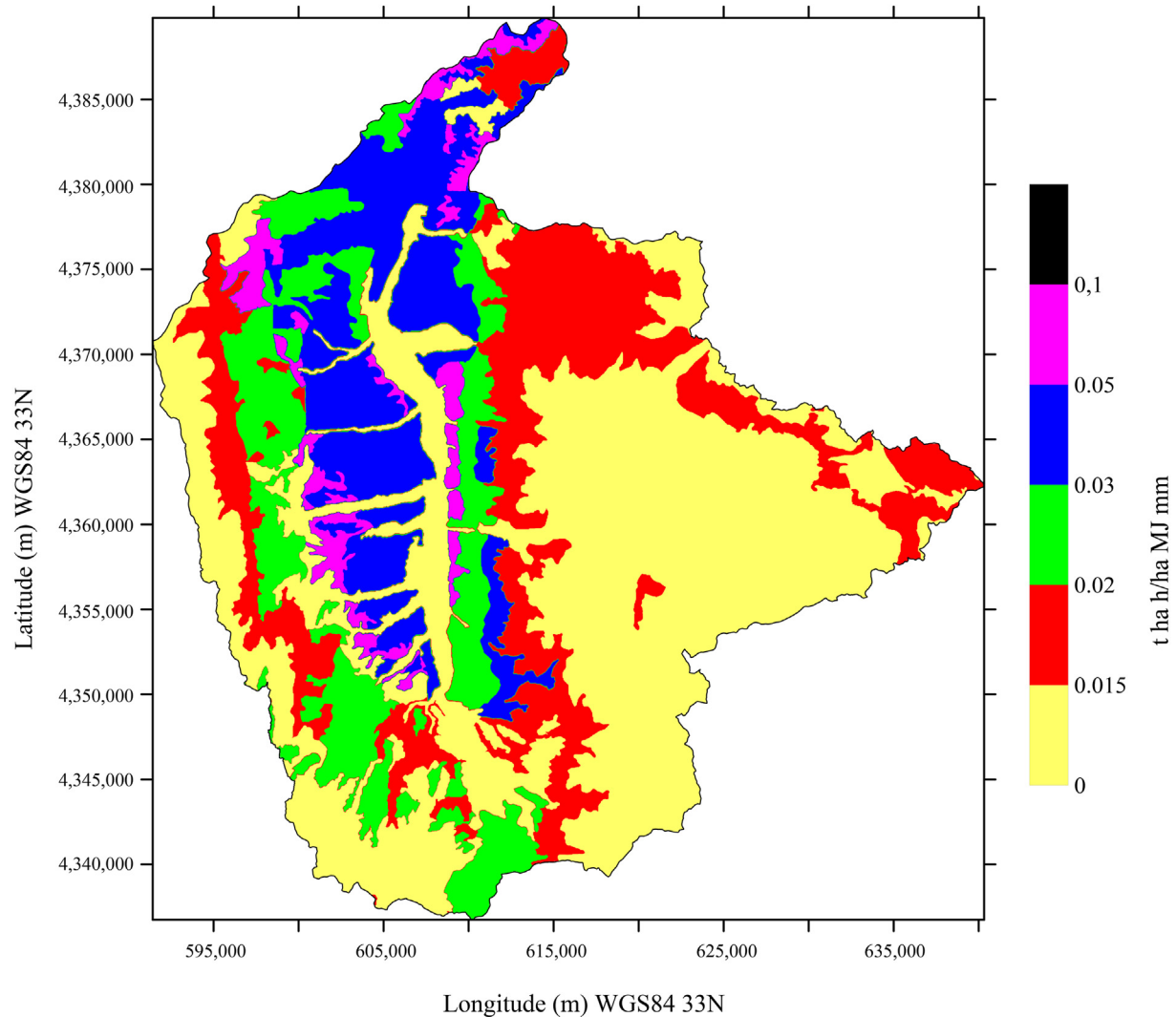


Fig. 5. Map of the soil erodibility factor K for the study area.

a common mesh size of 50 m. This procedure allowed a map of soil loss for the catchment area to be obtained for each land use scenario. The resulting maps are shown in Fig. 9 together with the mean values of soil loss related to the catchment area. In general, the maps show a large spatial variability of soil loss over the catchment area. However, it is worth noting that, the areas with higher values of soil loss can be identified in the hillslopes draining to the main course of the river or to the tributaries located in the Coastal Chain. On the contrary, the area covered by the Sila Plateau shows less vulnerability to soil erosion risk even if local situations, especially those associated with high values of the topographic factor in the eastern part of the catchment (see Fig. 6(a)), show higher risk. However, based on the mean value calculated for the catchment area and related to each land use scenario, the catchment experienced moderate to severe erosion risk (Zachar, 1982) especially for the land use scenario in 1977 (see Fig. 9).

4. Discussion

As previously indicated, the fallout radionuclide ^{137}Cs , utilized as sediment tracer, offers a considerable potential for providing general information on rates of overbank floodplain sedimentation within a catchment. The information reported in Table 2 provides a first

important indication on the rates of sediment deposition in the floodplain area of the Crati catchment for the two time windows 1963–2020 and 1986–2020. Table 2 also reports an attempt to estimate the deposition rate for the period 1954–2020 that can be deduced from Fig. 8 using, as a third marker horizon, the soil layer corresponding to the deepest horizon that shows the presence of ^{137}Cs activity (see Ritchie et al., 2004). Clearly this value is associated with a greater uncertainty than for that related to the other two marker horizons, because the ^{137}Cs flux related to the first years of the atmospheric fallout may now be under detection limits and these circumstances may produce a general underestimation of the sedimentation rates. However, looking at Fig. 8(c), that shows the depth distribution of ^{137}Cs with the highest activity, it is possible to identify a third peak below the 1963 marker horizon. Based on the global record up to 1987 summarized in Fig. 1, it can be deduced that this peak can be related to 1959 fallout and the assumption to identify the 1954 marker horizon a few centimeters below is plausible. Based on this last assumption, the three marker horizons made it possible to estimate deposition rates for three discrete time windows namely 1954–1963, 1963–1986, and 1986–2020. The results of these estimates are reported in graphical form in Fig. 10(a).

It is clear from Fig. 10(a) that the values obtained from the three sampling points show a decreasing trend of deposition rates

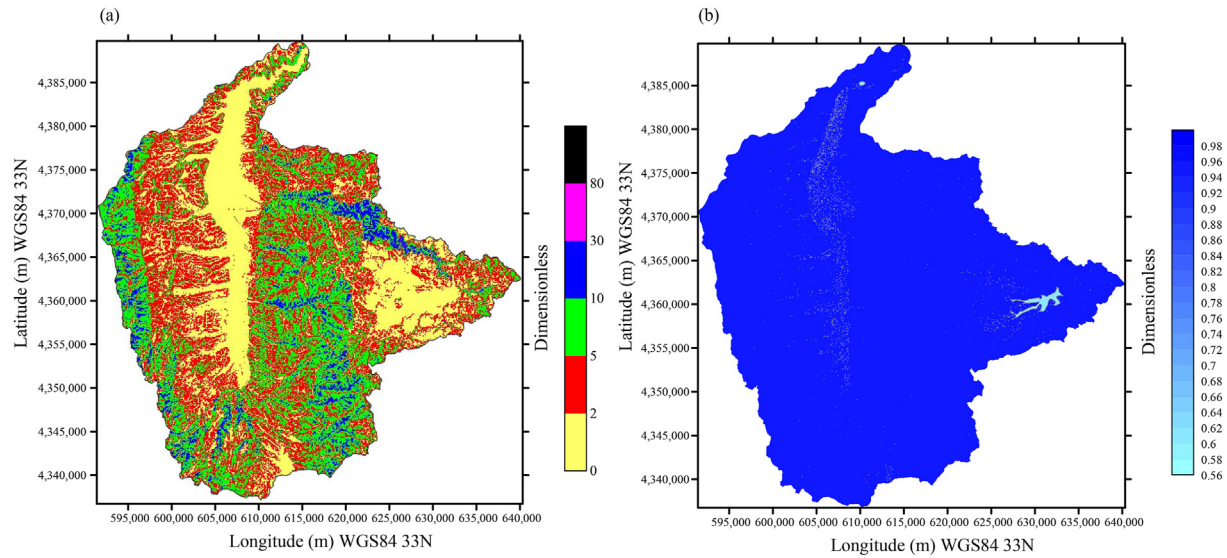


Fig. 6. Maps of the topographic factor LS (a) and of the support practice factor P (b) for the study area.

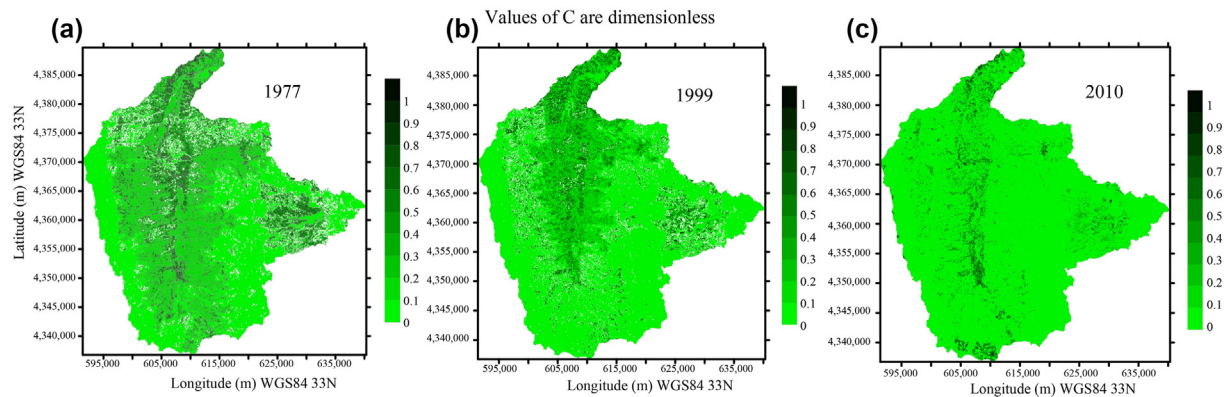


Fig. 7. Maps of the cover and management factor C for the study area related to three different years.

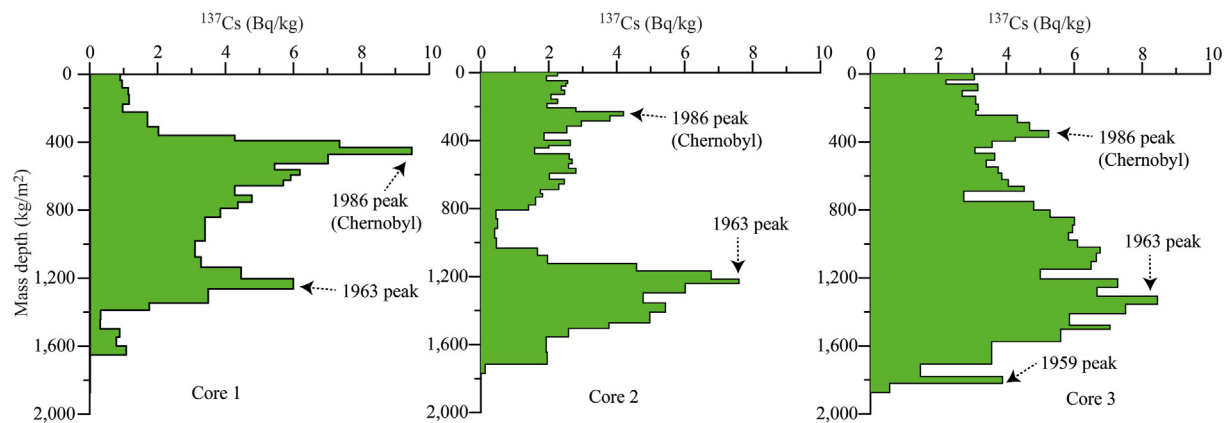


Fig. 8. Depth distribution of ^{137}Cs related to the three sampling points collected in the floodplain area.

providing a clear indication that the conservation strategies applied with the reforestation program produced a general reduction of the amount of sediment transported from the portions of the catchment located upstream of the floodplain area. Similar results were obtained by Ritchie et al. (2004) and Golosov et al. (2008) in two different contexts. Ritchie et al. (2004), in a study made in the Stemple Creek Watershed in northern California, documented a

general decrease of sediment deposition documented by ^{137}Cs sediment profiles in the floodplain areas as reflecting the change in land use that occurred in that area since the middle 1950s (mainly related to reduction in row crop agriculture and to an increase in pastureland). Golosov et al. (2008), in a study done on a small arable catchment in Russia, reported the results of deposition rates for two time windows: before and after the introduction of soil

Table 2
Deposition rates calculated within the floodplain area of the Crati catchment.

Sectioned core	Sedimentation rate (kg/(m ² ·y))		
	1954–2020	1963–2020	1986–2020
Site 1	24.94	22.08	13.76
Site 2	22.08	13.76	34.38
Site 3	13.76	34.38	43.03

(one order of magnitude). The authors explained these contrasting values by a rapid decrease of agricultural areas during the period 1990s–2000s and the occurrence of lower spring snowmelt flood peaks during the last several decades. The work of Moustakim et al. (2022), done in four cultivated lands in Morocco, showed that the net soil erosion rates have generally decreased due to some conservation measures consisting of a combination of more frequent fallow periods with natural vegetation and crop rotation practices.

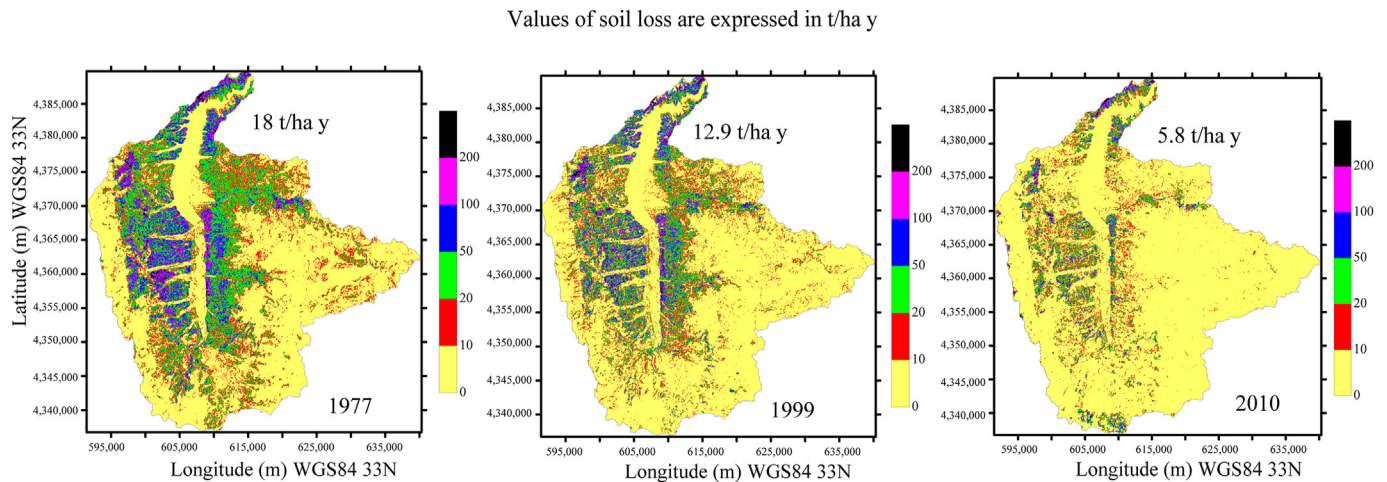


Fig. 9. Spatial distribution and mean values of soil loss provided by the RUSLE model for the catchment Crati for different land use scenarios.

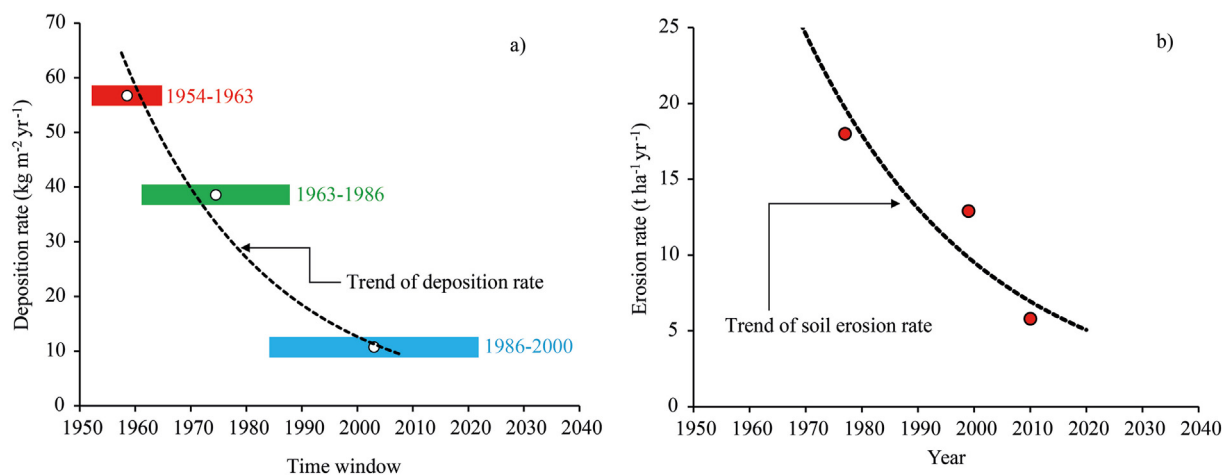


Fig. 10. Estimates of deposition rates for the three sampling points in the floodplain area (a) and estimates of soil loss of the catchment area provided by the RUSLE model for three different land use scenarios (b).

conservation measures (forest belts) in the upper part of the catchment. In that case, a small dam was built in the lower reach of the catchment at the same time as planting forest belts at the beginning of 1986. The authors found that the use of conservation measures led to decreases of soil loss rates by at least a factor of 2.5–2.8.

Other examples in which the ¹³⁷Cs sediment profiles in reservoirs or floodplain areas were used to detect changes in land use are reported by Belyaev et al. (2013b) and Moustakim et al. (2022). In the study of Belyaev et al. (2013b), a sedimentation rate of ca. 30 mm/y was estimated in the River Chern basin in Russia before 1964. At the same site, for the period after 1986 a value around 3 mm/y indicated a drastic decrease of the sediment deposition rate

In this case, the results obtained with the dating technique based on ¹³⁷Cs was combined with the ¹³⁷Cs resampling approach undertaken at the same sites. Even if the reduction of sedimentation rates is different depending on the geomorphic context, strategies utilized, and effect of climate change, it can be said that the results are in line with the findings of the aforementioned studies done in different areas of the world and they can be indicative of the positive impact of the reforestation.

In order to confirm this assumption, the estimates of soil loss obtained with the RUSLE model for the three different land use scenarios related to 1977, 1999, and 2010 are shown in Fig. 10(b) for comparison. Even in this case, the rates of soil erosion documented by the model show a very clear decreasing trend confirming once

again the reduction of soil loss over time reflecting the reforestation program operated during the period from the early 1950s to the late 1970s over the catchment area.

5. Conclusions

The combination of a dating technique provided by ^{137}Cs measurements on a floodplain area with estimates of soil loss derived from a distributed approach based on RUSLE proved to be very effective to evaluate the effect of land use change on soil loss and to provide important information on the impact of reforestation on soil erosion in this representative catchment. This strategy allowed a general decrease in soil erosion/deposition rates to be documented in this area of southern Italy and reflects the impact of the afforestation programs applied during the period from the early 1950s to the late 1970s in Calabria. As such, this strategy can be considered very useful to predict rates of soil erosion/deposition rates over large areas not covered by direct observations and should be seen as a useful tool to inform planners about the development of effective erosion and sediment control strategies in these areas. The current findings, also, highlight the importance of forest cover in influencing rates of soil loss in the study area and indicate the need to promote the use of reforestation to provide effective soil protection. However, further research is required to test this strategy in different geomorphic and climatic contexts in southern Italy and to give higher reliability to these preliminary results.

Declaration of competing interest

The authors declare that they have no known competing financial interests or personal relationships that could have appeared to influence the work reported in this paper.

Acknowledgements

This current study has been finalized in the frame of Erasmus + KA2 - Cooperation for Innovation and the Exchange of Good Practices - Capacity Building in the field of Higher Universities of Western Balkan Countries/SETOF. The authors are also indebted to the Agenzia Regionale per la Protezione dell'Ambiente della Calabria (ARPACAL) for providing rainfall data used in this study.

References

- Agenzia Regionale Servizi Sviluppo Agricolo (ARSSA). (2003). *I suoli della Calabria: Carta dei Suoli in scala 1:250000 della Regione Calabria*. Cosenza, Italy: Agenzia Regionale per lo Sviluppo e per i Servizi in Agricoltura in Calabria. (in Italian)
- Altieri, V., De Franco, S., Lombardi, F., Marziliano, P. A., Menguzzato, G., & Porto, P. (2018). The role of silvicultural systems and forest types in preventing soil erosion processes in mountain forests. A methodological approach using Caesium-137 measurements. *Journal of Soils and Sediments*, 18(12), 3378–3387.
- Amodio Morelli, L., Bonardi, G., Colonna, V., Dietrich, D., Giunta, G., Ippolito, F., Liguori, V., Lorenzoni, S., Paglionico, A., Perrone, V., Piccarreta, G., Russo, M., Scandone, P., Zanettin Lorenzoni, E., & Zuppetta, A. (1976). L'arco calabro-peloritano nell'orogene appenninico maghrebide. *Memorie della Società Geologica Italiana*, 17, 1–60. (in Italian)
- Arnaez, J., Lasanta, T., Errea, M. P., & Ortigosa, L. (2011). Land abandonment, landscape evolution, and soil erosion in a Spanish Mediterranean mountain region: The case of Camero Viejo. *Land Degradation & Development*, 22, 537–550.
- Belyaev, V. R., Golosov, V. N., Markelov, M. V., Evrard, O., Ivanova, N. N., Paramonova, T. A., & Shamshurina, E. N. (2013a). Using Chernobyl-derived ^{137}Cs to document recent sediment deposition rates on the River Plava floodplain (Central European Russia). *Hydrological Processes*, 27, 807–821.
- Belyaev, V. R., Golosov, V. N., Markelov, M. V., Evrard, O., Ivanova, N. N., & Shamshurina, E. N. (2013b). Effects of land use and climate changes on small reservoir siltation in the agricultural belt of European Russia (pp. 134–145). International Association of Hydrological Sciences. Publication No. 362.
- Capra, A., Porto, P., & La Spada, C. (2017). Long-term variation of rainfall erosivity in Calabria (Southern Italy). *Theoretical and Applied Climatology*, 128(1–2), 141–158.
- Cello, G., Tortorici, L., Turco, E., & Guerra, I. (1981). Profili profondi in Calabria settentrionale. *Bollettino della Società Geologica Italiana*, 100, 423–431. (in Italian)
- De Vincenzo, A., Molino, A. J., Molino, B., & Scorpio, V. (2017). Reservoir rehabilitation: The new methodological approach of Economic Environmental Defence. *International Journal of Sediment Research*, 32(2), 288–294.
- Di Stefano, C., Ferro, V., & Porto, P. (2000). Length slope factors for applying the Revised Universal Soil Loss Equation at basin scale in southern Italy. *Journal of Agricultural Engineering Research*, 75(4), 349–364.
- Di Stefano, C., Ferro, V., Porto, P., & Rizzo, S. (2005). Testing a spatially distributed sediment delivery model (SEDD) in a forested basin by caesium-137 technique. *Journal of Soil and Water Conservation*, 60(3), 148–157.
- D'ippolito, A., Ferrari, E., Iovino, F., Nicolaci, A., & Veltri, A. (2013). Reforestation and land use change in a drainage basin of southern Italy. *iForest: Biogeosciences and Forestry*, 6, 175–182.
- Formetta, G., Rago, V., Capparelli, G., Rigon, R., Muto, F., & Versace, P. (2014). Integrated physically based system for modeling landslide susceptibility. *Procedia Earth and Planetary Science*, 9, 74–82.
- Froehlich, W., & Walling, D. E. (2007). *The use of environmental radionuclides in investigations of sediment sources and overbank sedimentation rates in the Himalaya Foreland, India* (pp. 137–146). International Association of Hydrological Sciences. Publication No. 309.
- Golosov, V. N., Belyaev, V. R., Kuznetsova, J. S., Markelov, M. V., & Shamsurina, E. N. (2008). Response of a small arable catchment sediment budget to introduction of soil conservation measures. *International Association of Hydrological Sciences Publication No.*, 325, 106–113.
- Golosov, V. N., Belyaev, V. R., & Markelov, M. V. (2013). Application of Chernobyl-derived ^{137}Cs fallout for sediment redistribution studies: Lessons from European Russia. *Hydrological Processes*, 27, 781–794.
- He, Q., & Walling, D. E. (1996). Rates of overbank sedimentation on the flood plains of British lowland rivers documented using fallout ^{137}Cs . *Geografiska Annaler - Series A: Physical Geography*, 78a, 223–234.
- Hu, S., Gan, Z. M., & Yan, J. P. (2001). The impacts of urbanization on soil erosion in the Loess Plateau region. *Journal of Geographical Sciences*, 11, 282–290.
- Ispettorato Nazionale per la Sicurezza Nucleare (ISIN). (2021). *Attività nucleari e radioattività ambientale. Rapporto ISIN sugli indicatori. Il edizione 2021—Dati 2020*. Rome, Italy: Ispettorato nazionale per la sicurezza nucleare e la radio-protezione. (in Italian)
- Khodadadi, M., Zaman, M., Mabit, L., Blake, W. H., Gorji, M., Samani Bahrami, A., Meftahi, M., & Porto, P. (2020). Exploring the potential of using ^{7}Be measurements to estimate soil redistribution rates in semi-arid areas: Results from Western Iran and southern Italy. *Journal of Soils and Sediments*, 20(9), 3524–3536.
- Lal, R., & Moldenhauer, W. C. (1987). Effects of soil erosion on crop productivity. *Critical Reviews in Plant Sciences*, 5(4), 303–367.
- Lastoria, B., Simonetti, M. R., Casaioli, M., Mariani, S., & Monacelli, G. (2006). Socio-economic impacts of major floods in Italy from 1951 to 2003. *Advances in Geosciences*, 7, 223–229.
- Li, Z., & Fang, H. (2016). Impacts of climate change on water erosion: A review. *Earth-Science Reviews*, 163, 94–117.
- Maeda, E. E., Pellikka, P. K. E., Siljander, M., & Clark, B. J. F. (2010). Potential impacts of agricultural expansion and climate change on soil erosion in the Eastern Arc Mountains of Kenya. *Geomorphology*, 123(3–4), 279–289.
- McCool, D. K., Brown, L. C., Foster, G. R., Mutchler, C. K., & Meyer, L. D. (1987). Revised slope steepness factor for the universal soil loss equation. *Transactions of the American Society of Agricultural Engineers*, 30(5), 1387–1396.
- McCool, D. K., Foster, G. R., Mutchler, C. K., & Meyer, L. D. (1989). Revised slope length factor for the universal soil loss equation. *Transactions of the American Society of Agricultural Engineers*, 32(5), 1571–1576.
- Moore, I. D., & Burch, G. J. (1986). Modeling erosion and deposition: Topographic effects. *Transactions of the American Society of Agricultural Engineers*, 29, 1624–1630. 1640.
- Moustakim, M., Benmansour, M., Nouira, A., Benkdad, A., & Damnati, B. (2022). Caesium-137 re-sampling approach and excess Lead-210 sediment dating to assess the impacts of climate change and agricultural practices on soil erosion and sedimentation in Northwest Morocco. *Environmental Earth Sciences*, 81, 278.
- Moustakim, M., Benmansour, M., Zouagui, A., Nouira, A., Benkdad, A., & Damnati, B. (2019). Use of caesium-137 re-sampling and excess lead-210 techniques to assess changes in soil redistribution rates within an agricultural field in Nakhla watershed. *Journal of African Earth Sciences*, 156, 158–167.
- Nearing, M. A., Pruski, F. F., & O'neal, M. R. (2004). Expected climate change impacts on soil erosion rates: A review. *Journal of Soil and Water Conservation*, 59, 43–50.
- Ouadja, A., Benfetta, H., Porto, P., Flanagan, D. C., Mihoubi, M. K., Omeir, M. R., Graia, M., Ghosal, K., & Talchabhadel, R. (2021). Mapping potential soil erosion using RUSLE, remote sensing, and GIS: A case study in the watershed of Oued El Ardjem, Northwest Algeria. *Arabian Journal of Geosciences*, 14(18), 1945.
- Panagos, P., Standardi, G., Borrelli, P., Lugato, E., Montanarella, L., & Bosello, F. (2018). Cost of agricultural productivity loss due to soil erosion in the European union: From direct cost evaluation approaches to the use of macroeconomic models. *Land Degradation & Development*, 29(3), 471–484.
- Pimentel, D., Harvey, C., Resosudarmo, P., Sinclair, K., Kurz, D., McNair, M., Crist, S., Shpritz, L., Fitton, L., Saffouri, R., & Blair, R. (1995). Environmental and economic costs of soil erosion and conservation benefits. *Science*, 267(5201), 1117–1123.
- Porto, P. (2016). Exploring the effect of different time resolutions to calculate the rainfall erosivity factor R in Calabria, southern Italy. *Hydrological Processes*, 30, 1551–1562.
- Porto, P., Bacchi, M., Preiti, G., Romeo, M., & Monti, M. (2022). Combining plot measurements and a calibrated RUSLE model to investigate recent changes in

- soil erosion in upland areas in Southern Italy. *Journal of Soils and Sediments*, 22, 1010–1022.
- Porto, P., & Callegari, G. (2022). Comparing long-term observations of sediment yield with estimates of soil erosion rate based on recent ^{137}Cs measurements. Results from an experimental catchment in Southern Italy. *Hydrological Processes*, 36(9), e14663.
- Porto, P., & Walling, D. E. (2015). Use of caesium-137 Measurements and long-term records of sediment load to calibrate the sediment delivery component of the SEDD model and explore scale effect: Examples from Southern Italy. *Journal of Hydrologic Engineering*, 20(6), C4014005.
- Porto, P., Walling, D. E., & Callegari, G. (2009). Investigating the effects of afforestation on soil erosion and sediment mobilisation in two small catchments in Southern Italy. *Catena*, 79, 181–188.
- Porto, P., Walling, D. E., & Callegari, G. (2018). Using repeated ^{137}Cs and $^{210}\text{Pb}_{\text{ex}}$ measurements to establish sediment budgets for different time windows and explore the effect of connectivity on soil erosion rates in a small experimental catchment in Southern Italy. *Land Degradation & Development*, 29, 1819–1832.
- Porto, P., Walling, D. E., La Spada, C., & Callegari, G. (2016). Validating the use of ^{137}Cs measurements to derive the slope component of the sediment budget of a small catchment in southern Italy. *Land Degradation & Development*, 27, 798–810.
- Soil Survey Staff. (2014). Soil survey field and laboratory methods manual. In R. Burt and Soil Survey Staff (Ed.), *Soil Survey investigations report No. 51, version 2.0*. Lincoln, NE, USA: U.S. Department of Agriculture, Natural Resources Conservation Service.
- Renard, K. G., Foster, G. R., Yoder, D. C., & McCool, D. K. (1994). RUSLE revisited: Status, questions, answers, and the future. *Journal of Soil and Water Conservation*, 49(3), 213–220.
- Ritchie, J. C., Finney, V. L., Oster, K. J., & Ritchie, C. A. (2004). Sediment deposition in the flood plain of Stemple Creek Watershed, northern California. *Geomorphology*, 61, 347–360.
- Ritchie, J. C., Hawks, P. H., & McHenry, J. R. (1975). Deposition rates in valleys determined using fallout ^{137}Cs . *Geological Society of America Bulletin*, 86, 1128–1130.
- Ritchie, J. C., McHenry, J. R., & Gill, A. C. (1973). Dating recent reservoir sediments. *Limnology & Oceanography*, 18, 255–264.
- Robinson, D. A., & Blackman, J. D. (1990). Soil erosion and flooding: Consequences on land use policy and agricultural practice on the South Downs, East Sussex, UK. *Land Use Policy*, 7(1), 41–52.
- Romero-Díaz, A., Ruiz-Sinoga, J. D., Robledano-Aymerich, F., Brevik, E. C., & Cerdà, A. (2017). Ecosystem responses to land abandonment in Western Mediterranean Mountains. *Catena*, 149, 824–835.
- Sahli, Y., Mokhtari, E., Merzouk, B., Laignel, B., Vial, C., & Madani, K. (2019). Mapping surface water erosion potential in the Soummam watershed in Northeast Algeria with RUSLE model. *Journal of Mountain Science*, 16(7), 1606–1615.
- Scarciglia, F., Nicolaci, A., Del Bianco, S., Pelle, T., Soligo, M., Tuccimei, P., Marzaioli, F., Passariello, I., & Iovino, F. (2020). Reforestation and soil recovery in a Mediterranean mountain environment: Insights into historical geomorphic and vegetation dynamics in the Sila Massif, Calabria, southern Italy. *Catena*, 194, 104707.
- Senanayake, S., Pradhan, B., Huete, A., & Brennan, J. (2020). Assessing soil erosion hazards using land-use change and landslide frequency ratio method: A case study of Sabaragamuwa Province, Sri Lanka. *Remote Sensing*, 12, 1483.
- Shao, Z., Sumari, N. S., Portnov, A., Ujoh, F., Musakwa, W., & Mandela, P. J. (2021). Urban sprawl and its impact on sustainable urban development: A combination of remote sensing and social media data. *Geo-spatial Information Science*, 24(2), 241–255.
- Terranova, O., Antronico, L., Coscarelli, R., & Iaquina, P. (2009). Soil erosion risk scenarios in the Mediterranean environment using RUSLE and GIS: An application model for Calabria (southern Italy). *Geomorphology*, 112, 228–245.
- Thorntwaite, C. W. (1948). An approach toward a rational classification of climate. *Geographical Review*, 38, 55–94.
- Uddin, K., Matin, M. A., & Maharjan, S. (2019). Assessment of land cover change and its impact on changes in soil erosion risk in Nepal. *Sustainability*, 10, 4715.
- Vespasiano, G., Apollaro, C., Muto, F., Dotsika, E., De Rosa, R., & Marini, L. (2014). Chemical and isotopic characteristics of the warm and cold waters of the Lufiane Spa near Guardia Piemontese (Calabria, Italy) in a complex faulted geological framework. *Applied Geochemistry*, 41, 73–88.
- Wischmeier, W. H., Johnson, C. B., & Cross, B. V. (1971). A soil erodibility nomograph for farmland and construction sites. *Journal of Soil and Water Conservation*, 26, 189–193.
- Wischmeier, W. H., & Smith, D. D. (1978). *Predicting rainfall-erosion losses. A guide to conservation farming*. Beltsville, MD, USA: U.S. Department of Agriculture.. Agriculture Handbook, No. 537.
- Zachar, D. (1982). *Soil erosion. Developments in soil science 10*. Bratislava: Veda in co-edition with Amsterdam Elsevier.
- Zapata, F. (2002). *Handbook for the assessment of soil erosion and sedimentation using environmental radionuclides*. Dordrecht: Kluwer.